Supporting Information

Temperature Variation Induced Performance Decline of Perovskite Solar Cells

Jonas A. Schwenzer,* [†] *Lucija Rakocevic,* [‡,§] *Robert Gehlhaar,* [‡] *Tobias Abzieher,* [†] *Saba Gharibzadeh* [†], *Somayeh Moghadamzadeh* [†], *Aina Quintilla,* [#] *Bryce S. Richards,* [†,+] *Uli Lemmer,* [†,+] *and Ulrich W. Paetzold* [†,+,*]

[†] Light Technology Institute, Karlsruhe Institute of Technology, Engesserstr. 13, 76131 Karlsruhe, Germany

[‡] imec, Kapeldreef 75, 3001 Leuven, Belgium

[§] ESAT, KUL, Kastelpark Arenberg 10, 3000 Leuven, Belgium

[#] Center for Functional Nanostructures, Karlsruhe Institute of Technology, Wolfgang-Gaede-Str. 1a, 76131 Karlsruhe, Germany

[+] Institute of Microstructure Technology, Karlsruhe Institute of Technology, Hermann-von-Helmholtz-Platz 1, 76344 Eggenstein-Leopoldshafen, Germany

Corresponding Author

*E-mail: jonas.schwenzer@kit.edu

Theoretical Recapitulation of Temperature Effects in Solar Cells

The fundamental textbook equation that illustrates the temperature dependence of the V_{oc} as derived from the diode equation is[27]

$$\frac{\mathbf{d}\boldsymbol{V}_{\mathbf{OC}}}{\mathbf{d}\boldsymbol{T}_{\boldsymbol{C}}} = -\frac{\frac{\boldsymbol{E}_{\mathbf{g0}}}{\boldsymbol{e}} - \boldsymbol{V}_{\mathbf{OC}} + \boldsymbol{\gamma}\frac{\boldsymbol{k}_{\mathbf{B}}\boldsymbol{T}_{\mathbf{C}}}{\boldsymbol{e}}}{\boldsymbol{T}_{\mathbf{C}}} \sim const \quad \text{for} \quad 10\ °\mathrm{C} \leq \mathrm{T_C} \leq 60\ °\mathrm{C} \tag{1}$$

were

$$\boldsymbol{\gamma} = \mathbf{1} - \frac{\mathbf{d}\ \mathbf{ln}\ \boldsymbol{ERE}_{\mathbf{OC}}}{\mathbf{d}\ \mathbf{ln}\ \boldsymbol{T}_{\mathbf{C}}} + \left(\mathbf{2}\frac{\mathbf{d}\ \mathbf{ln}\ \boldsymbol{E}_{\mathbf{g}}}{\mathbf{d}\ \mathbf{ln}\ \boldsymbol{T}_{\mathbf{C}}} - \frac{\mathbf{d}\ \mathbf{ln}\ \boldsymbol{J}_{\mathbf{SC,1sun}}}{\mathbf{d}\ \mathbf{ln}\ \boldsymbol{T}_{\mathbf{C}}}\right) \sim const\ for\ 10\ °C \leq T_C \leq 60\ °C\ , \tag{2}$$

T_C is the temperature of the solar cell, E_{g0} is the bandgap at 0 K, k_B is the Boltzmann constant, e is the elementary charge*,* ERE_{OC} *is* external radiative efficiency, and $J_{SC,1sun}$ is the short-circuit current density at 1 sun incidence. Since the first two subtrahends in Equation (1) are small, compared to the third term, they can be neglected. Thus, taking into account that g is constant or can be neglected in the investigated temperature range;

The short-circuit current density (J_{SC}) depends on the ideal current $J_{SC,1sun}$ and the collection fraction (f_C):[25]

$$\boldsymbol{J}_{\mathbf{SC}}(\boldsymbol{T}_{\mathbf{C}}) = \boldsymbol{J}_{\mathbf{SC,1sun}}(\boldsymbol{T}_{\mathbf{C}})\boldsymbol{f}_{\mathbf{C}}(\boldsymbol{T}_{\mathbf{C}}) \tag{4}$$

$J_{SC,1sun}$ is a function of the bandgap of the semiconductor and the incident spectrum of the light. Usually, the bandgaps of most semiconductors such as Si and CIGS decrease with temperature thus leading to an increase in short-circuit current. However, in methylammonium lead iodide (MAPI) perovskites the bandgap increases with temperature.[29] Therefore, the ideal current is likely to decrease in these devices. It is noteworthy, that minor changes in E_g can have a high influence in the output current, measured with a solar simulator, if the bandgap is near a peak of the spectrum. The collection fraction is a function of the reflection, transmission, parasitic absorption and recombination of charge carriers in the solar cell. The temperature coefficient for J_{SC} can be extracted from equation (4) by deriving it in respect to temperature:

$$\boldsymbol{\beta_{J_{SC}}(T_{\mathrm{C}}) = \frac{1}{J_{\mathrm{SC}}(25\,^{\circ}\mathrm{C})}\frac{\mathrm{d}J_{\mathrm{SC}}}{\mathrm{d}T_{\mathrm{C}}} = \frac{1}{J_{\mathrm{SC}}(25\,^{\circ}\mathrm{C})}\frac{J_{\mathrm{SC,1sun}}}{\mathrm{d}E_{\mathrm{g}}}\frac{\mathrm{d}E_{\mathrm{g}}}{\mathrm{d}T_{\mathrm{C}}} + J_{\mathrm{SC,1sun}}(T_{\mathrm{C}})\frac{\mathrm{d}f_{\mathrm{C}}}{\mathrm{d}T_{\mathrm{C}}}} \tag{5}$$

For silicon based solar cells both terms of the sum in Equation (5) are positive, leading to an overall increase in J_{SC} with temperature. In contrast, at least the first term is negative for perovskite solar cells. The second term might be positive if the increased recombination rate is compensated by a reduction in other loss mechanisms. Nonetheless, we expect the overall sum to be negative, which means a reduction in short-circuit current with an increase in temperature.

Figure S1. Proof of stable power output of the investigated perovskite solar cells. (a) JV-characteristics of a solar cell prior and subsequent to ten hours of continuous illumination with an AM1.5 spectrum. (b) Stabilized power output of a perovskite solar cell prior and subsequent to 2.4 hours of illumination with an AM1.5 spectrum.

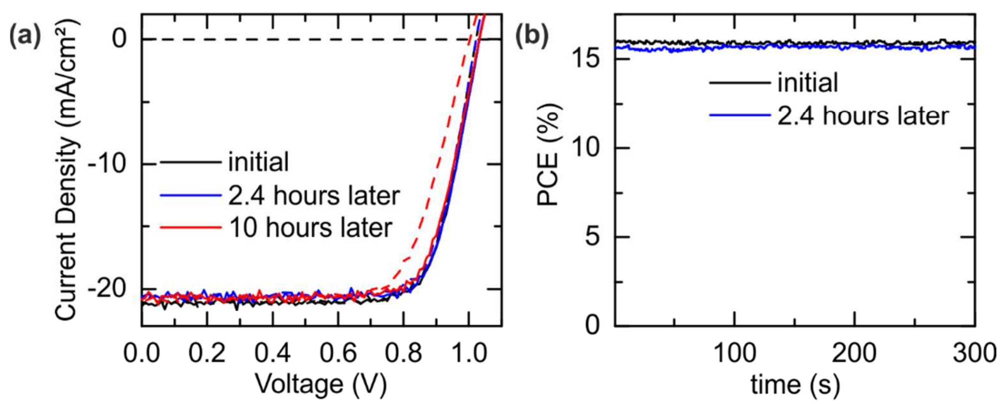

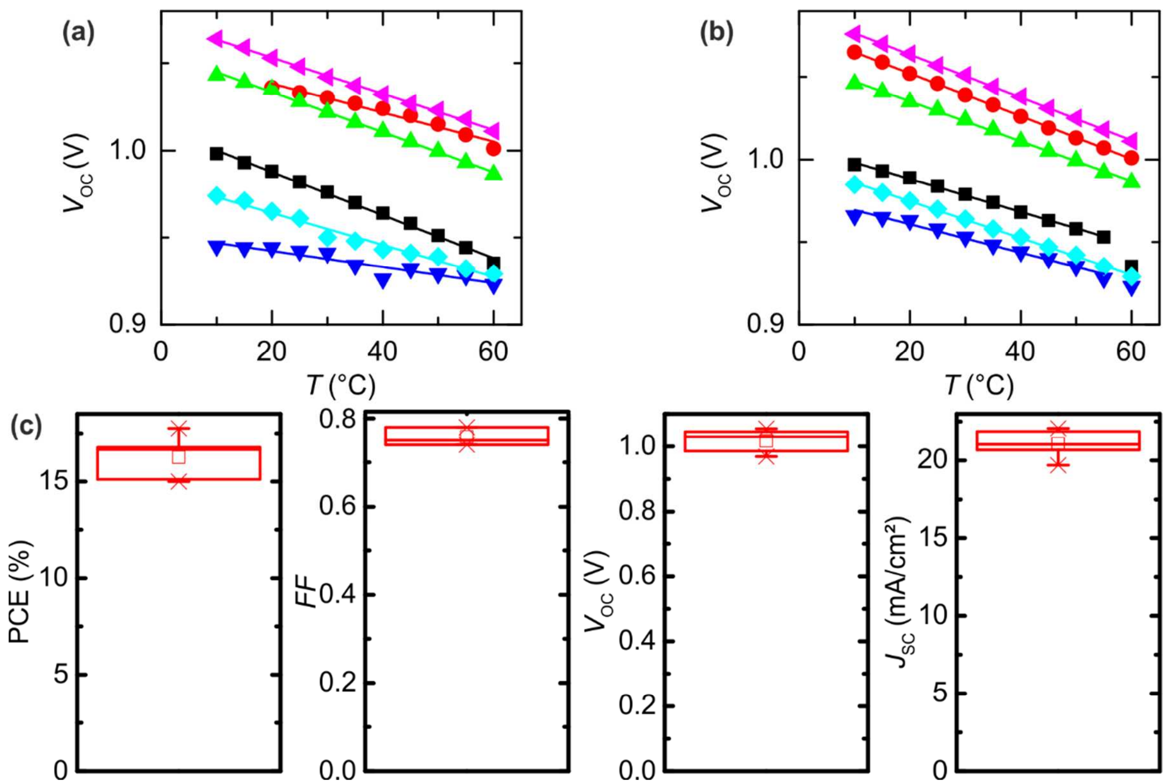

Figure S2. Open-circuit voltage (V_{OC}) as a function of temperature as extracted from the temperature cycles shown in Figure 1 with 7 min step time and 5 °C temperature steps for increasing temperature (a) and decreasing temperature (b). A linear fit to the data is shown. Different colors represent different solar cells. (c) Shows the performance parameters extracted from *JV* measurements.

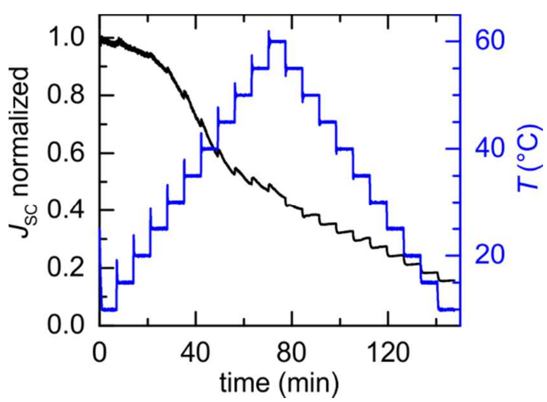

Figure S3. Normalized J_{sc} values of the PSC stressed with a temperature cycle which is presented in Figure 2b.

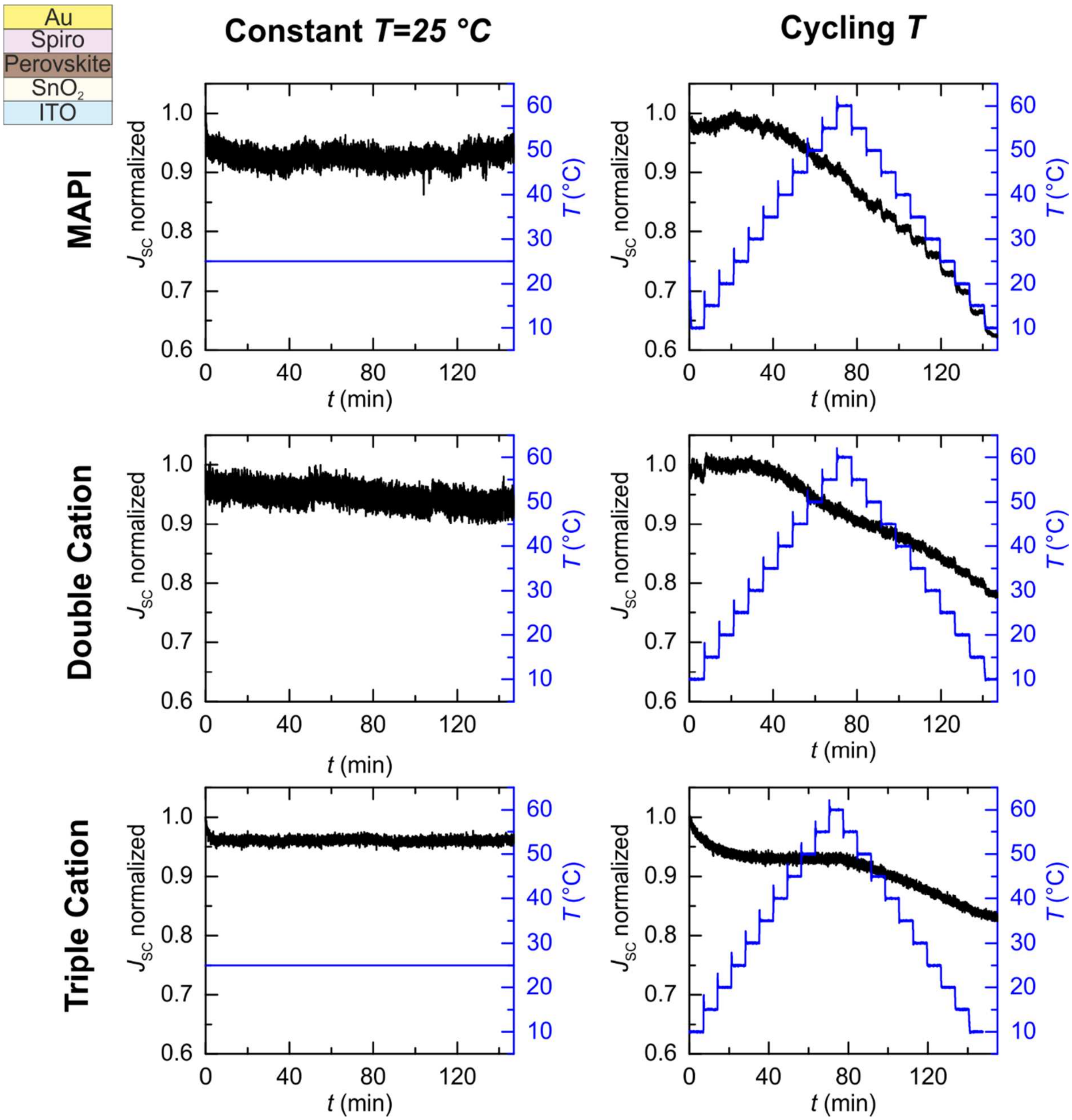

Figure S4. Short-circuit current measurements at constant temperature and with temperature cycles in PSCs with SnO_2 as electron transport layer and different perovskite absorber materials. The temperature variation induced current degradation is demonstrated for all investigated absorber materials.

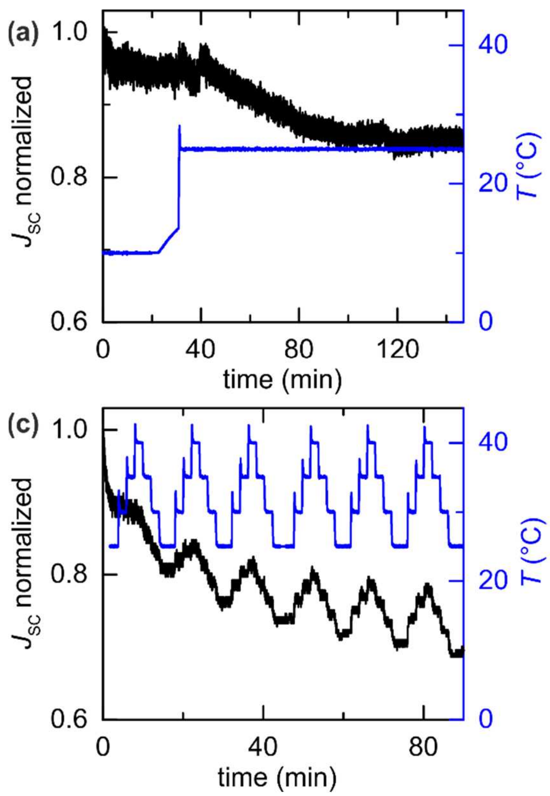

Figure S5. Short circuit current (J_{sc}) dependence of perovskite solar cells on the temperature dynamics. (a) The impact of one single temperature step on the J_{SC}. The short-circuit current stabilizes 40 minutes after changing the temperature. (b) Influence of the temperature range on the current degradation. (c) Influence of the temperature cycling speed on the degradation.

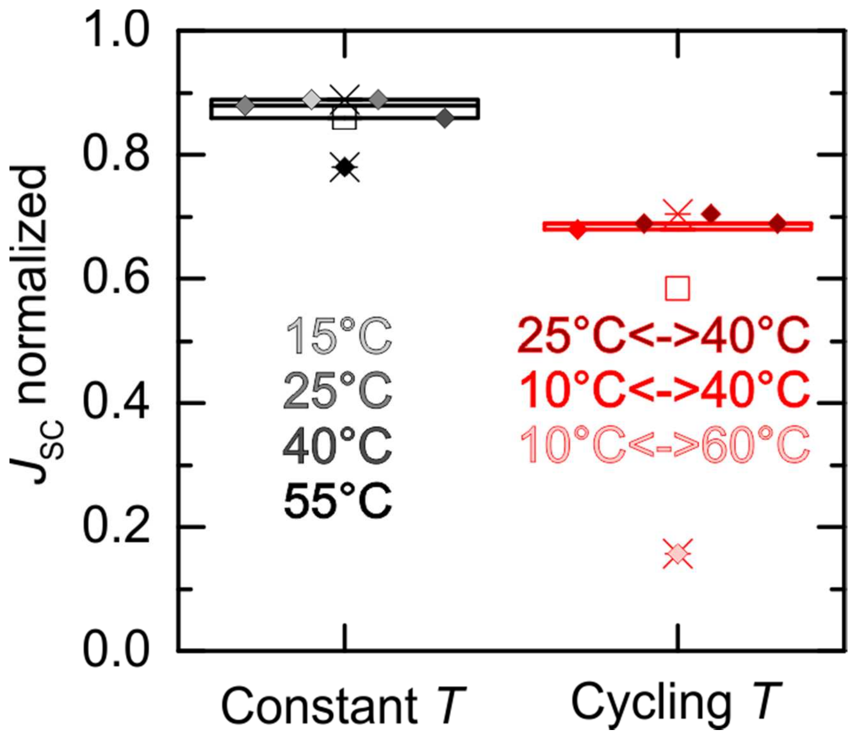

Figure S6. Statistics of end values of short-circuit current density measurements at various constant temperatures compared to temperature cycles showing the temperature variation induced current degradation.

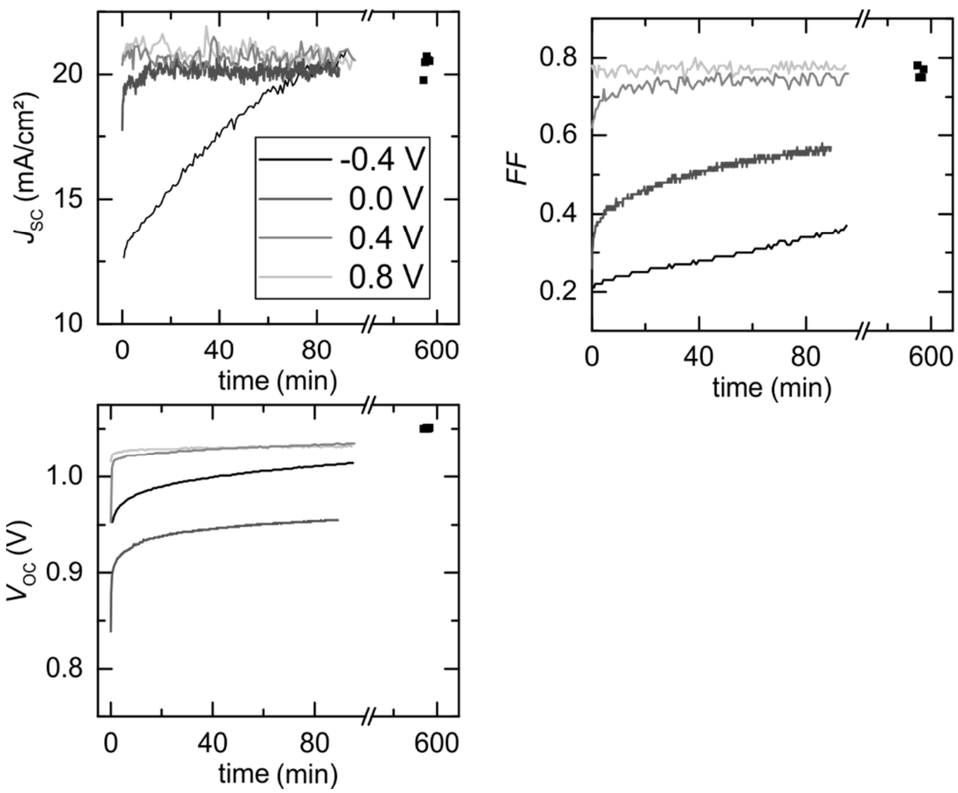

Figure S7. Recovery of the short-circuit current (J_{sc}), fill factor(FF), and open-circuit voltage (V_{OC}) of perovskite solar cells after the measurement at constant voltages with temperature cycles presented in Figure 3.

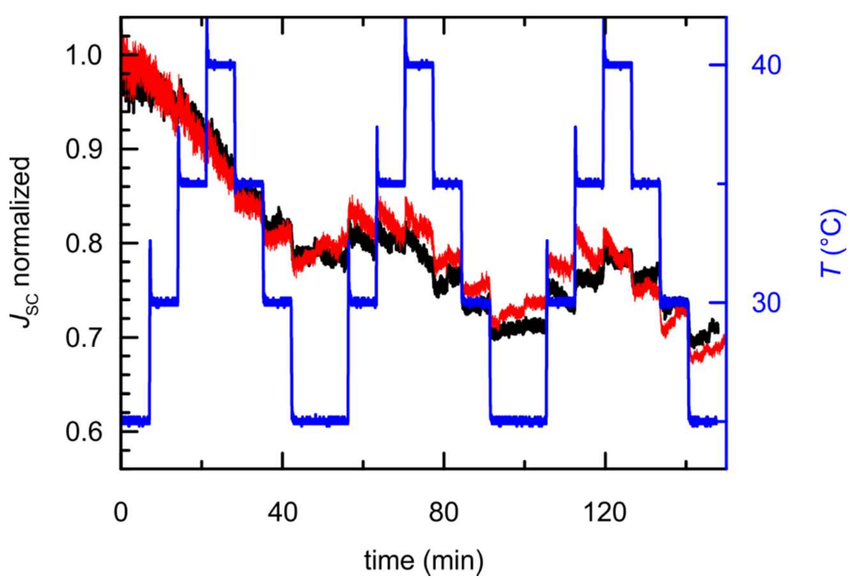

Figure S8. Reproducibility of the current degradation when temperature cycles are applied at short-circuit as shown by two measurements on different perovskite solar cells.

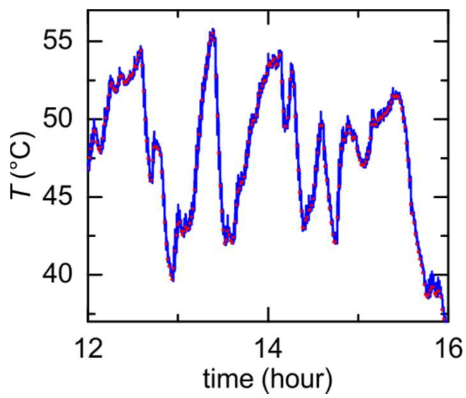

Figure S9. Comparison between the measured outdoor temperature profile and the replicated profile by the temperature controlled measurement holder.

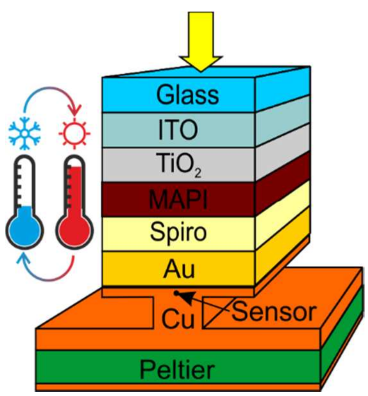

Figure S10. Scheme of the temperature controlled measurement setup. The peltier element is accessed via a microcontroller.

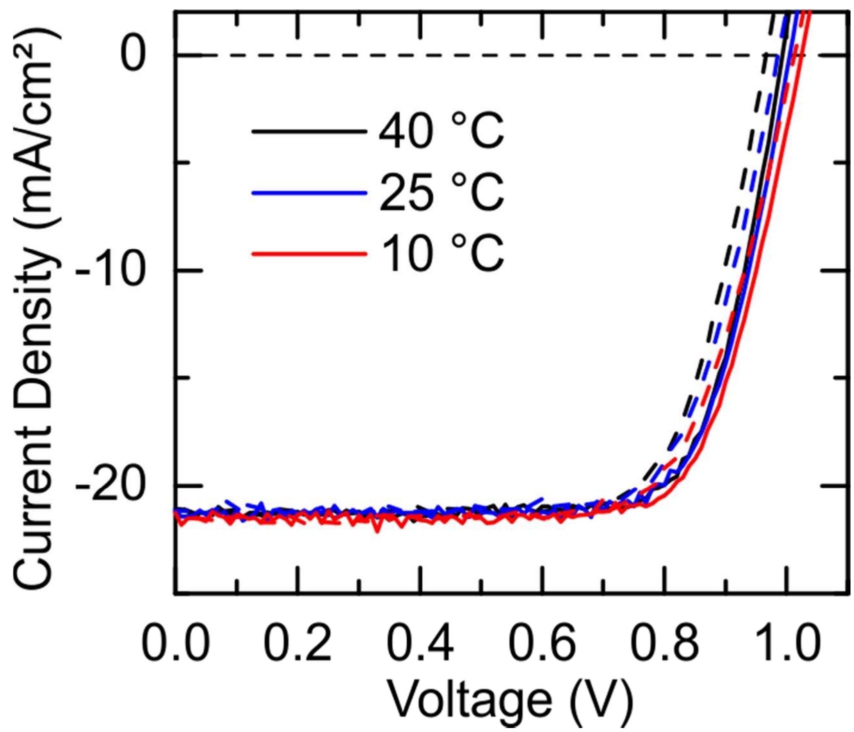

Figure S11. Current-Voltage characteristics in backward and forward direction of the investigated ITO/TiO_2/MAPI/Spiro-OMeTAD/Au architecture at different temperatures.

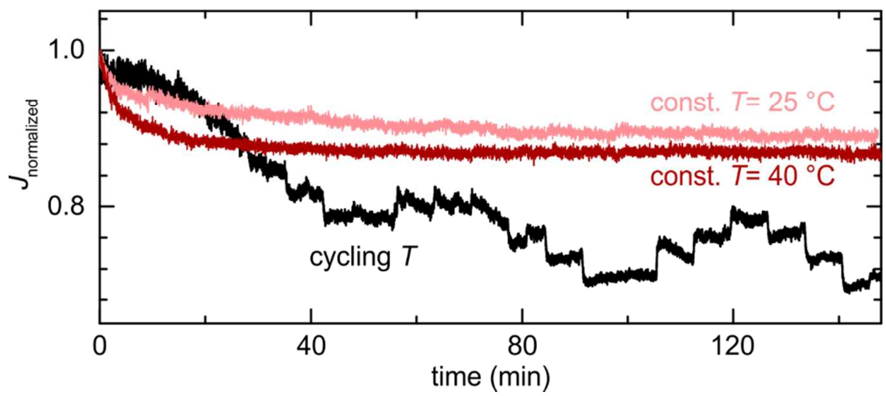

Figure S12. Temperature variation induced degradation in short-circuit current compared to the short-circuit current at constant temperatures.

Figure S13. Cross section SEM image of the PSCs used in this work. The architecture is glass(black)/ITO(blue)/TiO_2(yellow)/MAPI(green)/Spiro-OMeTAD(red)/gold(gold)